

## Electronic States of Toroidal Carbon Nanotubes

Ming-Fa LIN and Der-San CHUU<sup>1</sup>

*Department of Physics, National Cheng Kung University, Tainan, Taiwan 70101, The Republic of China*

<sup>1</sup>*Electrophysics Department, National Chiao Tung University, Hsinchu, Taiwan 30050, The Republic of China*

(Received July 16, 1997)

Toroidal carbon nanotubes (TCN's) are threaded by magnetic flux ( $\phi$ ). The magneto-electronic structures are studied within the tight-binding model. The curvature effect, which is due to the misorientation of the  $\pi$ -electron orbitals, might play an important role on the low energy electronic states. The thin TCN's, with armchair-zigzag and zigzag-armchair structures, exhibit four (three) types of energy gaps in the presence (absence) of the curvature effect. The magnetoelectronic structures clearly vary with  $\phi$  except the thin zigzag-armchair TCN's. They could exhibit the periodical Aharonov-Bohm oscillations, since the Zeeman splitting is generally negligible except at large  $\phi$ 's.

KEYWORDS: electronic states, toroidal carbon nanotubes, tight-binding model

### §1. Introduction

Since carbon nanotubes were discovered in 1991 by Iijima,<sup>1)</sup> they have attracted a lot of attention. One of the most interesting properties is that the electronic properties are mainly determined by their geometric structures.<sup>2-8)</sup> Each straight carbon nanotube (SCN) is a graphite sheet which is rolled up in the cylindrical form. Its radius ( $r$ ) is only between 10 and 150 Å, while its length is more than 1  $\mu$ m. Carbon nanotubes could bend within the crystalline rope,<sup>9)</sup> and the two ends are found to be able to knit together seamlessly.<sup>10)</sup> Hence carbon atoms could form a toroidal carbon nanotube (TCN, or a carbon toroid), with an average radius  $R \sim 1500 - 2500$  Å. The toroid radius is much larger than the height or the width ( $2r \sim 10$  Å), i.e., a TCN is very thin. Also noticed that armchair nanotubes ( $(m, m)$  nanotubes in Fig. 1) are shown to be the principal constituents of the crystalline rope, so they are the precursors of TCN's.<sup>10)</sup> Here we mainly study the electronic states of TCN's. The dependence on the geometric structure, the magnetic flux ( $\phi$ ), the curvature effect, and the Zeeman splitting is taken into account.

The toroidal forms of graphitic carbons could be built from nanotubes by: (1) bending a long nanotube and connecting its ends together (this work), (2) connecting small sliced parts of the nanotubes,<sup>11)</sup> and (3) connecting two sections of identical turnover bilayer nanotube ends at the equator of the resulting toroid.<sup>12)</sup> The carbon toroids constructed from the last two methods are not found in experiments up to now. Moreover, there are certain pentagons and heptagons instead of hexagons, and the ratio  $R/r$  is typically smaller than 10.<sup>11, 12)</sup> Hence their geometric structures are different from those studied in this work.

The geometric and electronic structures of SCN's, which are closely related to those of TCN's, are simply reviewed. A SCN is formed by rolling a graphite sheet in such a fashion that the atom at the origin coincides

with another atom at  $\mathbf{R}_x = m\mathbf{a}_1 + n\mathbf{a}_2$ , where  $\mathbf{a}_1$  and  $\mathbf{a}_2$  are the primitive lattice vectors of a graphite sheet (Fig. 1). A  $(m, n)$  SCN is predicted to be a metal or a semiconductor, which depends on the radius and the chiral angle about the axis.<sup>2-8)</sup> If the curvature effect due to the misorientation of the  $\pi$ -electron orbitals is neglected, SCN's with  $2m + n \neq 3i$  ( $i$  is an integer) are semiconductors, and the others are metals. But for a very small SCN, such an effect might play an important role on the low energy electronic structures.<sup>3, 8)</sup> SCN's could exhibit three types of electronic structures in the inclusion of the curvature effect. That is, a  $(m, n)$  SCN is (1) a moderate-gap semiconductor for  $2m + n \neq 3i$  (energy gap  $E_g \propto 1/r$ ), (2) a metal for  $m = n$  ( $E_g = 0$ ), and (3) a narrow-gap semiconductor for  $2m + n = 3i$  and  $m \neq n$  ( $E_g \propto 1/r^\alpha$ , where  $\alpha \geq 2$ ). The curvature effect is thus expected to be not negligible for a very thin TCN. The magnetoelectronic structures of SCN's, which exist in a uniform magnetic field parallel or perpendicular to the tubular axis, are detailedly studied by Ajiki and Ando.<sup>5)</sup> They would exhibit the periodical Aharonov-Bohm (AB) oscillation with magnetic flux in the absence of Zeeman effect.

A TCN corresponds to a finite graphite sheet rolled from the origin to the vectors  $\mathbf{R}_x$  and  $\mathbf{R}_y (= p\mathbf{a}_1 + q\mathbf{a}_2)$  simultaneously (Fig. 1). The parameters  $(m, n, p, q)$ , therefore, uniquely define a TCN. We mainly focus on the TCN's, which have the armchair structures along the transverse direction and the zigzag structures along the longitudinal direction, and vice versa. These two kinds of TCN's are called armchair-zigzag ( $(m, m, -p, p)$ ) and zigzag-armchair ( $(m, 0, -p, 2p)$ ) nanotubes separately.

The tight-binding model<sup>13)</sup> is used to study the  $\pi$ -electron states. It is similar to that employed for a graphite sheet, but with the periodical boundary conditions along the transverse ( $\parallel \mathbf{R}_x$ ) and the longitudinal ( $\parallel \mathbf{R}_y$ ) directions taken into account. A TCN thus owns a lot of discrete states characterized by the transverse ( $J$ ) and the longitudinal ( $L$ ) angular momenta. The low en-

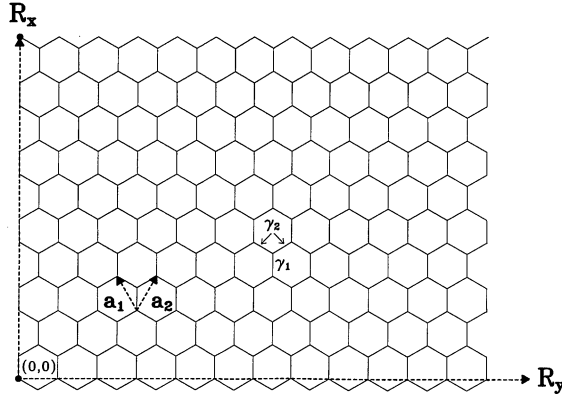


Fig. 1. A straight carbon nanotube could be regarded as a graphite sheet rolled from the origin to the vector  $\mathbf{R}_x = m\mathbf{a}_1 + n\mathbf{a}_2$ . When the origin further coincides with the vector  $\mathbf{R}_y = p\mathbf{a}_1 + q\mathbf{a}_2$ , a toroidal carbon nanotube is formed.  $\mathbf{a}_1$  and  $\mathbf{a}_2$  are the primitive vectors of a graphite sheet.

ergy electronic structures, as seen in SCN's,<sup>2-8)</sup> strongly depend on the geometric structures, such as width and radius. For thin TCN's, there are four (three) types of energy gaps at  $\phi = 0$  in the presence (absence) of the curvature effect (see §3). TCN's might have an energy gap between the highest occupied states (HOS) and the lowest unoccupied states (LUS). Moreover, only type II and type III TCN's have energy gaps which would vary with magnetic flux through TCN's. The  $\phi$ -dependent electronic structures of these two types of TCN's are detailedly investigated. They could drastically change from a semiconductor to a metal (or vice versa) at certain  $\phi_a$ 's, where both HOS and LUS touch the Fermi level  $E_F = 0$  simultaneously. In general, the Zeeman splitting is negligible except at large  $\phi$ , because the toroid radius is very large. The  $\phi$ -dependent electronic states would exhibit a periodical AB oscillation, with a period  $\phi_0$ .

This paper is organized as follows. In §2, the  $\pi$ -electron states of TCN's are calculated from the tight-binding model. The dependence on the geometric structure, the magnetic flux, the curvature effect, and the Zeeman splitting is discussed in §3. Concluding remarks are made in §4.

## §2. The Tight-Binding Model

A TCN could be regarded as a rolled-up graphite sheet

in the toroid form; that is, it needs to satisfy the periodical boundary conditions along the transverse and the longitudinal directions. The  $(m, m, -p, p)$  armchair-zigzag TCN's and the  $(m, 0, -p, 2p)$  zigzag-armchair TCN's are here chosen for a detailed study.

The magnetoelectronic structure of a TCN, as done for a graphite sheet,<sup>13)</sup> is calculated by the tight-binding model. A TCN here exists in a uniform perpendicular  $B$  field. The gauge  $\mathbf{A} = \mathbf{B} \times \mathbf{R}/2$  ( $\parallel \mathbf{R}_y$ ) is chosen such that the wave vector  $\mathbf{k} = -i\nabla + (e/c\hbar)\mathbf{A}$ .  $\mathbf{R}$  is the vector from the center to the surface of the toroid. Since TCN's are very thin, the vector potential at the toroid surface could be approximated as a constant  $\phi/2\pi R$ . Under such gauge, the periodical boundary conditions along the transverse and the longitudinal directions are

$$\begin{aligned}\Psi(\mathbf{r}) &= \Psi(\mathbf{r} + \mathbf{R}_x) \\ &= \Psi(\mathbf{r} + \mathbf{R}_y),\end{aligned}\quad (1)$$

where  $\Psi(\mathbf{r})$  is the Bloch function. For an armchair-zigzag (zigzag-armchair) TCN, the transverse and the longitudinal wave vectors obtained from eq. (1), respectively, are  $k_x = 2\pi J/3bm$  and  $k_y = 2\pi(L + \phi/\phi_0)/\sqrt{3}bp$  ( $k_x = 2\pi J/\sqrt{3}bm$  and  $k_y = 2\pi(L + \phi/\phi_0)/3bp$ ).  $b = 1.42 \text{ \AA}$  is the C-C bond length. The angular momenta  $J = 1, 2, \dots, m$  and  $L = 1, 2, \dots, p$  could serve as the state index.  $(J_a, L_a)$  is defined as the state nearest to the Fermi level ( $E_F = 0$ ).

For a TCN, there exist curvature along the transverse direction and bending along the longitudinal direction. The curvature effect, as predicted from the study on a small SCN,<sup>3,8)</sup> would affect the low energy electronic structure, but the bending effect is negligible. For example, for a zigzag nanotube with radius  $5 \text{ \AA}$  and length  $1 \mu\text{m}$ , the energy gaps due to curvature and bending are  $\sim 0.1 \text{ eV}$  and  $10^{-7} \text{ eV}$  respectively.<sup>3)</sup> The  $\pi$ -electron orbitals are not perfectly aligned due to the curvature, which, thus, leads to the small fluctuations of the bond hopping strength. The resonance integrals ( $\gamma_1$  and  $\gamma_2$  in Fig. 1) along the different directions might differ slightly. Diagonalizing the Hamiltonian with only the nearest-neighbor interactions, the  $\pi$ -electron state energies of TCN's are given by

$$E(J, L, \sigma, \phi) = E(J, L, \phi) + E(\sigma, \phi), \quad (2a)$$

where

$$E(J, L, \phi)_{\text{zig-arm}} = \pm \left\{ \gamma_1^2 \pm 4\gamma_1\gamma_2 \cos \left[ \frac{\pi J}{m} \right] \cos \left[ \frac{\pi(L + \phi/\phi_0)}{p} \right] + 4\gamma_2^2 \cos^2 \left[ \frac{\pi J}{m} \right] \right\}^{\frac{1}{2}}, \quad (2b)$$

$$E(J, L, \phi)_{\text{arm-zig}} = \pm \left\{ \gamma_1^2 \pm 4\gamma_1\gamma_2 \cos \left[ \frac{\pi J}{m} \right] \cos \left[ \frac{\pi(L + \phi/\phi_0)}{p} \right] + 4\gamma_2^2 \cos^2 \left[ \frac{\pi(L + \phi/\phi_0)}{p} \right] \right\}^{\frac{1}{2}}, \quad (2c)$$

and

$$E(\sigma, \phi) = \frac{g\sigma}{m^*R^2} \frac{\phi}{\phi_0}. \quad (2d)$$

+ and - signs appearing outside the square-root sign, respectively, correspond to the antibonding states (the  $\pi^*$  states) and the bonding states (the  $\pi$  states). On the

other hand, + and - signs inside the square-root sign are the unfolded and folded states, respectively.<sup>4)</sup>  $E(\sigma, \phi)$  is the spin- $B$  interaction. The  $g$  factor is taken to be the same with that ( $\simeq 2$ ) of graphite.<sup>14)</sup>  $\sigma = \pm 1/2$  is the electron spin, and  $m^*$  is the bare electron mass. The spin- $B$  interaction  $E(\sigma, \phi)$  could be neglected except at large  $\phi$ , e.g.,  $E(\sigma, \phi) \sim 10^{-6} \text{ eV}$  for the  $(5, 5, -5001, 5001)$

TCN at  $\phi = \phi_0$ . The two main effects due to the  $B$ -field are to change the angular momentum from  $L$  to  $L + \phi/\phi_0$  and induce the Zeeman splitting. Also noticed that the Fermi energy keeps vanishing during the variation of  $\phi$ , mainly owing to the symmetric  $\pi$ -electronic structure.

Kane and Mele have derived the analytic forms of the resonance integrals.<sup>8)</sup>  $\gamma_1 = \gamma_0$  and  $\gamma_2 = (1 - 3b^2/32r^2)\gamma_0$  for a zigzag SCN, and  $\gamma_1 = (1 - b^2/8r^2)\gamma_0$  and  $\gamma_2 = (1 - b^2/32r^2)\gamma_0$  for an armchair SCN.  $\gamma_0$  is the nearest-neighbor resonance integral in the absence of the curvature effect.<sup>4)</sup> They will be used to study the magnetoelectronic structures of the thin armchair-zigzag and zigzag-armchair TCN's. In addition, energy gaps of zigzag nanotubes are predicted to scale as  $1/r^2$ . Such gaps might be much larger than those obtained by Hamada *et al.*<sup>3)</sup> For example, energy gaps of the (6, 0), (9, 0) and (12, 0) nanotubes are 177.6 meV, 78.9 meV and 44.4 meV in ref. 8, but 200 meV, 40 meV and 8 meV in ref. 3. There exists considerable discrepancy for nanotubes with larger  $r$ 's, which might need further examinations.

### §3. Electronic States of Toroidal Carbon Nanotubes

We first see the electronic states in the absence of the curvature effect. At  $\phi = 0$ , there are three types of electronic structures. There exist simple relations between energy gaps and geometric structures. A type I TCN, which is characterized by  $E_g \sim b\gamma_0/r$ , corresponds to  $2m + n \neq 3i$ . It is a zigzag-armchair TCN, with a large gap. Its energy gap is the same with that of a large-gap SCN. For example,  $E_g \sim 0.5\gamma_0$  for the (7, 0, -5001, 10002) TCN and the (7, 0) SCN. A type II TCN, which exhibits  $E_g = 0$ , corresponds to  $2m + n = 3i$  and  $2p + q = 3i$ . It is a metal; that is, the HOS and LUS meet up with each other at  $E_F = 0$ . For example, the ( $J_a = 5$ ,  $L_a = 3334$ ) states of the (5, 5, -5001, 5001) TCN (the dashed curve in Fig. 2) would touch the Fermi level. Such type of TCN is an armchair-zigzag or zigzag-armchair TCN. A type III TCN defined by  $E_g = b\gamma_0/R$  (eq. (3a)) corresponds to  $m = n$  and  $2p + q \neq 3i$ . It has a small gap, *e.g.*,  $E_g \sim 7 \times 10^{-4}\gamma_0$  for the (5, 5, -5000, 5000) TCN (the solid curve in Fig. 2). It belongs to an

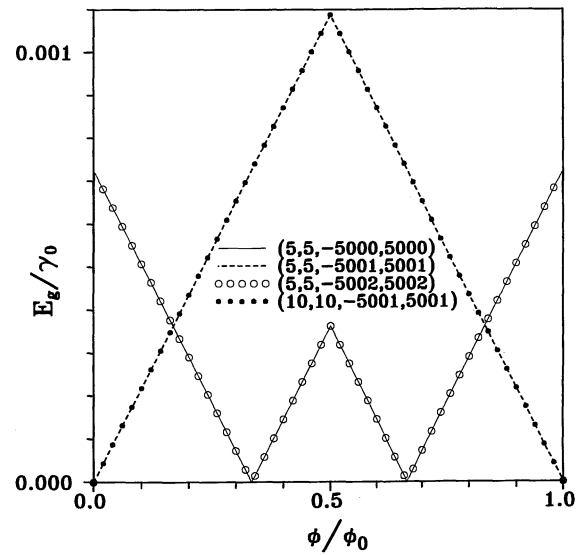


Fig. 2. The smallest energy difference between the highest occupied state and the lowest unoccupied state is periodical in magnetic flux. The results without the curvature effect are shown for four toroidal carbon nanotubes: (5, 5, -5000, 5000), (5, 5, -5001, 5001), (5, 5, -5002, 5002), and (10, 10, -5001, 5001).

armchair-zigzag TCN.

The low energy electronic structure of a  $(m, n, p, q)$  TCN could be understood from that of a  $(m, n)$  SCN. A TCN samples the  $\pi$ -electron states of a SCN, which satisfies the longitudinal periodical boundary condition. When a SCN is a metal, the edge state of the linear  $J_a$  subband would touch the Fermi level. If a TCN could (couldn't) sample such a state, it would exhibit the metallic (semiconducting) behavior. Metals or semiconductors are principally determined by the geometric structures. For example, a TCN, with  $2m + n = 3i$  and  $2p + q = 3i$ , is a gapless system in the absence of the curvature effect.

Electronic structures of type II and III TCN's are sensitive to magnetic flux, but the opposite is true for type I TCN's. The smallest energy differences, as calculated from eqs. (2b) and (2c) with  $\gamma_1 = \gamma_2 = \gamma_0$ , are given by

$$E_g(\phi) = \begin{cases} \frac{3b\gamma_0}{R} \frac{\phi}{\phi_0} & \text{for } 2m + n = 3i \text{ and } 2p + q = 3i. \\ \frac{3b\gamma_0}{R} \left| \frac{\phi}{\phi_0} - \frac{1}{3} \right| & \text{for } 2m + n = 3i \text{ and } 2p + q \neq 3i, \end{cases} \quad (3a)$$

$$E_g(\phi) = \begin{cases} \frac{3b\gamma_0}{R} \frac{\phi}{\phi_0} & \text{for } 2m + n = 3i \text{ and } 2p + q = 3i. \\ \frac{3b\gamma_0}{R} \left| \frac{\phi}{\phi_0} - \frac{1}{3} \right| & \text{for } 2m + n = 3i \text{ and } 2p + q \neq 3i, \end{cases} \quad (3b)$$

$E_g(\phi)$  is shown in Fig. 2 for type II and III TCN's. The energy gap is a linearly periodical function of  $\phi$ , with a period  $\phi_0$ ; moreover, it is symmetric about  $\phi_0/2$ . When  $\phi$  through a TCN varies, the electronic structure would change from a metal into a semiconductor or vice versa. The type II and III TCN's are metals at  $\phi_a = i\phi_0$  and  $(i \pm 1/3)\phi_0$  respectively.  $E_g(\phi)$  is inversely proportional to the toroid radius (eqs. (3a) and (3b)), but independent of the toroid height or width. For example, the (5, 5, -5001, 5001), (10, 10, -5001, 5001) (the solid circles), and (9, 0, -2887, 5774) (not shown) TCN's have the same  $E_g(\phi)$ . But on the other hand, the dependence on

the geometric structures would become very complicated in the presence of the curvature effect, as seen in Fig. 3.

When the curvature effect is further taken into account, there are four types of thin TCN's at  $\phi = 0$ . They include type I TCN's with  $E_g \sim \gamma_0 b/r$ , type II TCN's with  $E_g \sim 0$ , type III TCN's with  $E_g \sim \gamma_0 b/R$ , and type IV TCN's with  $E_g \sim 3\gamma_0 b^2/16r^2$ . Only type I and IV TCN's have a simple relation between energy gaps and geometric structures. These two types of TCN's belong to zigzag-armchair TCN's. A type I TCN, as seen in the absence of the curvature effect, corresponds to  $2m + n \neq 3i$ , *i.e.*, the curvature effect hardly alters the

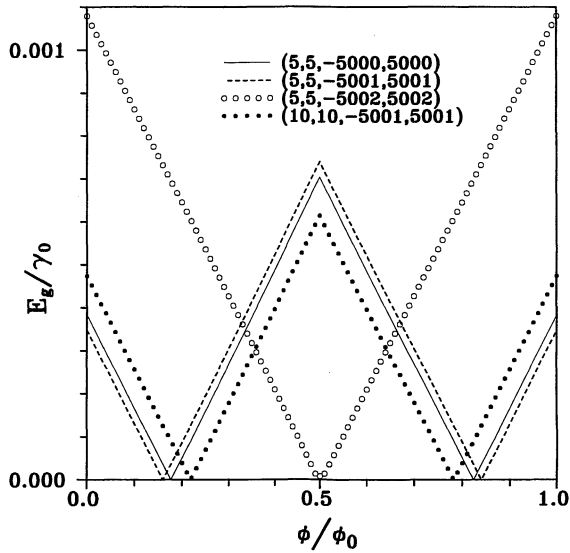


Fig. 3. Same plot as Fig. 2, but the curvature effect is taken into account. The inset shows the details at  $E_g \sim 0$  for the (5, 5, -5002, 5002) TCN.

large-gap characteristic. This type of TCN is apparently independent of magnetic flux. As for a type IV TCN, it corresponds to  $m = 3i$  and  $n = 0$ . The curvature effect has changed a thin  $(3i, 0, -p, 2p)$  TCN from a metal into a semiconductor. From eq. (2b), the energy gap related to the  $(J_a = 2m/3, L_a = p)$  state is given by

$$E_g(\phi) = 2\gamma_0 \left[ \left( \frac{3b^2}{32r^2} \right)^2 + \left( 1 - \frac{3b^2}{32r^2} \right) \frac{9b^2\phi^2}{4R^2\phi_0^2} \right]^{1/2}. \quad (4)$$

If the  $3b^2/32r^2$  terms caused by the curvature effect are neglected, eq. (4) is restored to eq. (3a). The energy gap is basically independent of magnetic flux for a thin TCN ( $r < 5 \text{ \AA}$ ). It suggests that the low-frequency physical

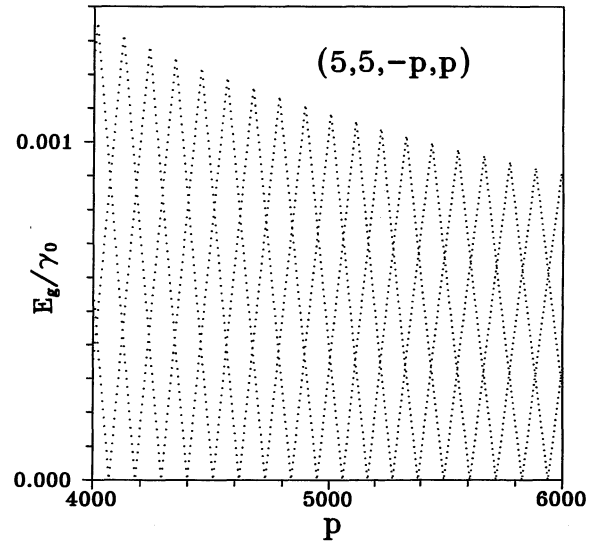


Fig. 4. The relation between the energy gap at  $\phi = 0$  and the geometric structures is shown for the various (5, 5, -p, p) TCN's.

properties, such as persistent currents,<sup>15)</sup> in thin TCN's are insensitive to magnetic flux. Energy gap at  $\phi = 0$  would quickly decrease in the increasing of height. Furthermore, it could exhibit a periodical oscillation with magnetic flux. A  $(3i, 0, -p, 2p)$  TCN, with a large height, is expected to be a small-gap semiconductor (similar to a type III TCN) or a vanishing-gap metal (a type II TCN). How high it would exhibit the metallic behavior requires a further study. The curvature effect on the resonance integrals, as stated earlier for  $(3i, 0)$  zigzag SCN's, is needed for such a study.

For thin TCN's, both type II and type III TCN's are  $(m, m, -p, p)$  armchair-zigzag TCN's. From eq. (2c), the energy gap of an armchair-zigzag TCN is given by

$$E_g(\phi) = 2\gamma_0 \left| \left( 1 - \frac{b^2}{8r^2} \right) \pm 2 \left( 1 - \frac{b^2}{32r^2} \right) \cos \left[ \frac{\pi(L_a + \phi/\phi_0)}{p} \right] \right| = \frac{3\gamma_0 b}{R} \left( 1 - \frac{b^2}{32r^2} \right) \left| \frac{\phi}{\phi_0} - \frac{\phi_a}{\phi_0} \right|. \quad (5)$$

As a result of the curvature effect angular momentum  $L_a$  and magnetic flux  $\phi_a$ , which correspond to  $E_g(\phi_a) = 0$  in eq. (5), are generally not equal to  $2p/3$  (or  $2p/3 \pm \phi_0/3$ , or  $p/3 \pm \phi_0/3$ ) and  $i\phi_0$  (or  $(i \pm 1/3)\phi_0$ ) respectively. It is thus difficult to directly obtain the energy gap from the geometric structures. That is to say, the simple rule,  $p = 3i$  or  $\neq 3i$ , in eqs. (3a) and (3b) is not available in distinguishing the magnetoelectronic structures of armchair-zigzag TCN's. The curvature effect has changed many of  $(m, m, -3i, 3i)$  TCN's from type II metals into type III semiconductors, *e.g.*, the (5, 5, -5001, 5001) (the dashed curve) and (10, 10, -5001, 5001) (the solid circles) TCN's in Fig. 3. It would make the energy gap depend on the toroid height. For example, the (5, 5, -5001, 5001) and (10, 10, -5001, -5001) TCN's have the different energy gaps. Furthermore, it significantly affects the energy gaps of TCN's with the almost same radii. For example, energy gaps of the (5, 5, -5000, 5000) (the solid curve) and (5, 5, -5002, 5002) TCN's

(the open circles) quite differ from each other.

The relation between the energy gap at  $\phi = 0$  and the geometric structures deserves a closer examination. The energy gaps of the various (5, 5, -p, p) TCN's, as seen in Fig. 4, strongly depend on the geometric structures. Most of armchair-zigzag TCN's belong to type III TCN's with  $E_g \sim \gamma_0 b/R$ . Only a little TCN's have the energy gaps which are much smaller than  $\gamma_0 b/R$  ( $E_g < 10^{-5}\gamma_0$ ). Moreover, the latter might be an armchair characterized by  $p \neq 3i$ , *e.g.*,  $E_g \sim 5 \times 10^{-6}\gamma_0$  for the (5, 5, -5827, 5827) TCN. It further illustrates that there is no simple rule in distinguishing semiconductors and metals from the geometric structures. In general, an armchair-zigzag TCN could not sample the edge state of an armchair SCN, since the wave vector of such a state shifts slightly from  $2\sqrt{3}\pi/9b$  due to the curvature effect.<sup>2,3,8)</sup> This reason could explain the aforementioned results. In short, the curvature effect plays an important role in the low energy electronic structures of thin armchair-zigzag

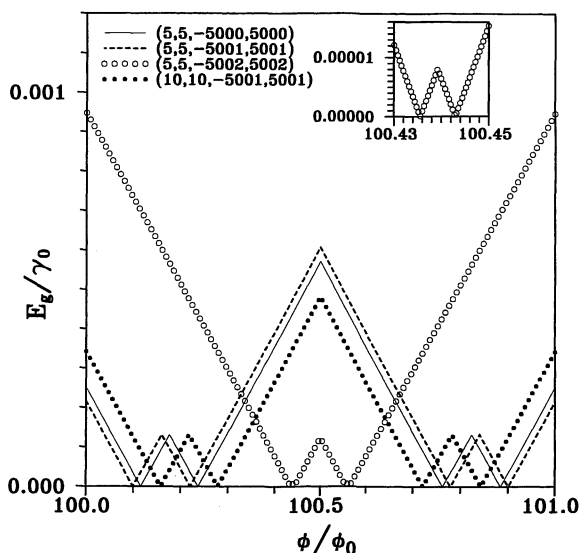


Fig. 5. Same plot as Fig. 2, but with the curvature effect and the Zeeman splitting taken into account. The inset shows the details at  $E_g \sim 0$  for the (5, 5, -5002, 5002) TCN.

TCN's, which is in great contrast to that in small armchair SCN's.<sup>2,3,8)</sup>

The spin- $B$  interaction,  $E(\sigma, \phi)$  in eq. (2d), needs to be taken into consideration at large  $\phi$ , *e.g.*,  $\phi \sim 100\phi_0$ . The energy gaps at  $100\phi_0 \leq \phi \leq 101\phi_0$  are shown in Fig. 5 for various armchair-zigzag TCN's. Compared with that in Fig. 3, the periodicity of the AB oscillation is clearly destroyed by the inclusion of the spin- $B$  interaction, *e.g.*,  $E_g(0) = E_g(\phi_0) \neq E_g(100\phi_0)$ . The energy of the spin-down state becomes lower, while that of the spin-up state becomes higher. Consequently the Zeeman splitting would make certain states touch the Fermi level at magnetic flux smaller and larger than  $\phi_a$  in eq. (5). The metal-semiconductor transitions would happen relatively frequently. Hence the Zeeman splitting is expected to have a strong effect on magnetic properties at large  $\phi$ , *e.g.*, the persistent currents.<sup>15)</sup>

#### §4. Concluding Remarks

The magnetoelectronic structures of thin TCN's are studied within the tight-binding model. The curvature effect and the Zeeman splitting are included in the calculations. The curvature effect might play an important role on the low energy electronic structures.

TCN's, with armchair-zigzag and zigzag-armchair

structures, exhibit four (three) types of energy gaps in the presence (absence) of the curvature effect. The electronic structures would vary with  $\phi$  except the thin zigzag-armchair TCN's. They could exhibit the periodic AB oscillation, since the Zeeman splitting is generally negligible except at large  $\phi$ 's. The metal-semiconductor transitions would happen during the variation of  $\phi$ . They are expected to cause interesting phenomena in the low-frequency physical properties, *e.g.*, the persistent currents and the electronic specific heat.<sup>15)</sup>

There are simple relations between the geometric structures and the electronic structures for thin zigzag-armchair TCN's. They do not exist for thin armchair-zigzag TCN's, if the curvature effect is taken into consideration. However, the geometric structures are closely related to the electronic structures and thus the low-frequency physical properties.

#### Acknowledgments

This work was supported in part by the National Science Council of Taiwan, the Republic of China under the Grant Nos. NSC 87-2112-M-006-019 and NSC 87-2112-M-009-009.

- 1) S. Iijima: *Nature* **354** (1991) 56; S. Iijima and T. Ichihashi: *Nature* **363** (1993) 603.
- 2) J. W. Mintwire, B. I. Dunlap and C. T. White: *Phys. Rev. Lett.* **68** (1992) 631.
- 3) N. Hamada, S. I. Sawada and A. Oshiyama: *Phys. Rev. Lett.* **68** (1992) 1579.
- 4) R. Saito, M. Fujita, G. Dresselhaus and M. S. Dresselhaus: *Appl. Phys. Lett.* **60** (1992) 2204; *Phys. Rev. B* **46** (1992) 1804; R. Saito, G. Dresselhaus and M. S. Dresselhaus: *Phys. Rev. B* **50** (1994) 14698.
- 5) H. Ajiki and T. Ando: *J. Phys. Soc. Jpn.* **62** (1993) 2470; *ibid.* **62** (1993) 1255; *ibid.* **63** (1994) 4267; *ibid.* **64** (1995) 260; *ibid.* **64** (1995) 4382; *ibid.* **65** (1996) 505.
- 6) J. P. Lu: *Phys. Rev. Lett.* **74** (1995) 1123.
- 7) X. Blase, L. X. Benedict, E. L. Shirley and S. G. Louie: *Phys. Rev. Lett.* **72** (1994) 1878.
- 8) C. L. Kane and E. J. Mele: *Phys. Rev. Lett.* **78** (1997) 1932.
- 9) A. Thess *et al.*: *Science* **273** (1996) 438.
- 10) J. Liu, H. Dai, J. H. Hafner, D. T. Colbert, R. E. Smalley, S. J. Tans and C. Dekker: *Nature* **385** (1997) 780.
- 11) B. I. Dunlap: *Phys. Rev. B* **46** (1992) 1933.
- 12) S. Itoh *et al.*: *Phys. Rev. B* **47** (1993) 1703; *ibid.* **47** (1993) 12908; *ibid.* **48** (1993) 8323; *ibid.* **49** (1994) 13970.
- 13) P. R. Wallace: *Phys. Rev.* **71** (1947) 622.
- 14) M. S. Dresselhaus and G. Dresselhaus: *Adv. Phys.* **30** (1981) 139.
- 15) M. F. Lin and D. S. Chuu: unpublished.